

Real-Time Adaptive Intelligent FPGA-based Back-Stepping Control Law Design for a Nonlinear Magnetic Ball Levitation System

Khulood E. Dagher

Al-Khwarizmi College of Engineering, University of Baghdad, Baghdad, Iraq
dagherkhulood@kecbu.uobagdad.edu.iq

Abstract: A new proposal for an adaptive intelligent Field Programmable Gate Array (FPGA) back-stepping nonlinear control law equation design and implementation for a strong nonlinear Magnetic ball Levitation (MagLev) system is introduced in this study. The aim of the suggested adaptive controller is to retain and stabilize the position of the magnetic ball to be suspended in a desired position within the magnetic field. The on-line Intelligent Bat Optimization (IBO) algorithm is used to find and tune the positive gain variables of the proposed adaptive control law based on Lyapunov method. These gain variables are used to obtain a suitable voltage action for the nonlinear system. The adaptive back-stepping technique is implemented by using FPGA Kit based on the schematic design of the Xilinx development tool Integrated Software Environment (ISE) with a high level programming language which named the Verilog. This language is used for testing the on line operation of the adaptive intelligent FPGA-Back-Stepping controller. The numerical simulation results along with the experimental work illustrate the improved performance of the proposed adaptive intelligent FPGA-back-stepping controller in terms of error reduction for the magnetic ball position and the smooth voltage control action. These results were confirmed by a comparative study with different nonlinear controller types.

Key words: Adaptive back-stepping method, FPGA-Kit, Intelligent Bat Optimization (IBO) algorithm, integrated software environment, magnetic levitation system, MATLAB package, LabVIEW package

INTRODUCTION

The Magnetic Levitation (MagLev) is a contemporary technology which has been applied in various industrial applications such as high-speed rail transportation, magnetic frictionless bearings, vibration isolation system and fast tool servo system. In concept, MagLev uses the magnetic force to move a magnetic object in the magnetic field or keeps it in a fixed position (Qin *et al.*, 2014). Recently, many works have been reported in the literature for various types of controllers and tuning control methodologies to solve the problem of the magnetic ball stabilization in a desired position for the MagLev system. They are focused on controller design based on the mathematical model of the physical nonlinear MagLev system such as: the Fuzzy PID (FPID) controller which was proposed by Trisanto *et al.* (2006) using on-line training neural networks to compensate for inadequate FPID parameters and for stabilizing the MagLev system. In addition, an intelligent adaptive back-stepping control system using a Recurrent Neural Network (RNN) to control the magnetic ball position of a MagLev system was proposed by Lin *et al.* (2007). The control objective was to obtain the best transient control performance and

robustness to uncertainties for the tracking of trajectories. The observer feedback controller was proposed by Baranowski and Piatek (2012) for estimating the velocity of the magnetic ball instead of a derivative in PID control of the position in order to improve the control quality and extend the range of system's stable operation. The improved adaptive fuzzy back-stepping control for a magnetic levitation system with uncertain parameters and structure was proposed by Sadek *et al.* (2017) to control the nonlinear magnetic ball's position by using symbiotic organism search optimization algorithm to initialize the adaptive and control parameters. A new model-free adaptive design approach which uses an adaptive-fuzzy procedure based on feedback linearization with the proposed rules was applied to the magnetic system without identification model to keep the position error close to zero. This method was explained by Javadi and Pezeshki (2013). By Muresan *et al.* (2015) the researchers proposed Riemann surface and a proper mapping in the w-plane methodology for designing and tuning a fractional order controller for a class of unstable MagLev systems. Moreover, an adaptive technique and sliding mode control schemes based Lyapunov stability theorem were developed by Boonsatit and Pukdeboon (2016) for

the control problem of a MagLev system to guarantee finite-time reachability of a given desired ball position. The cognitive on-line auto-tuning control algorithm with the back-stepping technique was used for the MagLev system in order to find the optimal voltage or current control action in the real-time system and to reduce the position error of the magnetic ball (Al-Araji, 2016). In addition, the Runge-Kutta Model Predictive Control (RKMPC) and the Field-Programmable Gate Array (FPGA) were used for the real-time experimental electromagnetic levitation system as proposed by Iplikci and Bahtiyar (2016). By Rubio *et al.* (2017) the researchers presented the angular position of the ball model and the combination of a nonlinear method based Lyapunov method with a neural network control of the MagLev system. Also, by Qin *et al.* (2014) the researchers presented a hybrid model based on a Radial Basis Function (RBF) neural networks with functional weights that are built the modeling of the magnetic levitation ball system then using linearized Model Predictive Controller (MPC) to achieve stable levitating and output-tracking control of the steel ball in the electromagnetic field.

The motivation for this research is to design and implement digital adaptive intelligent back-stepping control law based on Lyapunov method, so as to obtain the best voltage action for improving the performance of a real-time nonlinear MagLev system by using the proposed an adaptive intelligent digital control law equation based FPGA technique.

The list below shows the summarized new contributions of this study through a comparative study with different nonlinear controller types. A swift voltage control action which is generated using MATLAB simulation based on the proposed design of the nonlinear adaptive control law with Lyapunov criterion stability and intelligent bat optimization which leads to track and stabilize the steel magnetic ball in the desired position within the magnetic field with minimum tracking position error. Adaptive nonlinear back-stepping control law is designed, implemented and verified in a real-time by using FPGA-development Kit type Xilinx-Virtex-5 and simulated by Verilog programming language using Xilinx ISE 14.5 Version after replacing the proposed continuous control law equation by the proposed an adaptive intelligent digital control law equation.

To implement the proposed adaptive intelligent control law methodology in the FPGA-development Kit, there are three design steps. Firstly, the adaptive back-stepping control law equation is derived. Secondly, the control gain parameters of the adaptive control law equation is obtained and tuned using IBO algorithm to find the best control voltage signal that tracks the desired

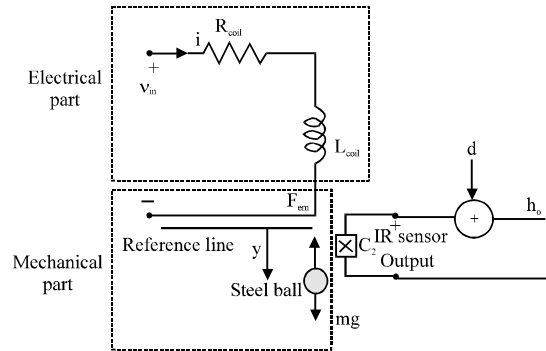


Fig. 1: Magnetic levitation model diagram

ball position of the magnetic levitation system based on the mean square of error performance specification. Thirdly, the proposed continuous adaptive control law equation is replaced by the adaptive intelligent digital control law equation based on the bilinear z-transform and it is implemented by using the Xilinx development tool with ISE Ver.14.5 and the performance and efficiency of the designed adaptive intelligent digital controller are demonstrated via. experimental results.

From the numerical MATLAB simulation results and experimental research, the position of the magnetic ball with respect to step position change, a fast excellent response without any overshoot and with a zero steady-state error was obtained because the adaptive intelligent digital control action has fast and smooth action with no spikes and oscillations compared with other nonlinear controller results in terms of the transient response and the steady-state error as well as the number of fitness evaluation as Al-Araji (2016), Abu Elreesh and Hamed (2012), Pati *et al.* (2016) and Ghosh *et al.* (2014).

Nonlinear system description: The MagLev Model is a one dimensional system which has a strong unstable nonlinear dynamics behaviour. The schematic diagram of the system can be observed in Fig. 1.

In general, the MagLev system consists of two parts which are used to describe the mathematical model as explained below (Muresan *et al.*, 2015; Pati *et al.*, 2016):

The first part: It is called an electrical model as it is identified by the operation of the magnetic ball levitation based on the magnetic field control voltage which depends on the value of the input current in the single-out electromagnetic coil inductance L_{coil} and resistance R_{coil} circuit of the system, hence, this model limits the position of the magnetic ball. The mathematical model of the first part can be described as:

Table 1: The physical parameters (Pati *et al.*, 2016; Ghosh *et al.*, 2014)

Parameters	Values
Control input voltage level (v_{in})	-5 to 5 V
Magnetic ball mass (m)	0.02 kg
Constant of magnetic force (k_{mf})	$kg.m^3/sec^2/A^2$
Constant of gravitation (g)	9.81 m/sec ²
Control voltage to the coil current gain (C_1)	0.95 A/V
IR sensor gain (C_2)	143.48 V/m
Offset voltage (d)	-2.8 V
Output voltage level (h_o)	(-3.75 to 1.25) V

$$v_{in}(t) = R_{coil}i(t) + L_{coil} \frac{di(t)}{dt} \quad (1)$$

Where:

i = The variable input current value applied to the electromagnetic coil

v_{in} = The variable voltage control action

Therefore, the current $i(t)$ flows in the coil and is proportional to the voltage $v_{in}(t)$ and can be expressed as given in Eq. 2 for the MagLev 33-201 feedback instrument Ltd., model which has the physical parameters illustrated in Table 1 (Pati *et al.*, 2016; Ghosh *et al.*, 2014):

$$i(t) = C_1 \times v_{in}(t) \quad (2)$$

where, C_1 is the control voltage to the coil current gain.

The second part: It represents the mechanical model that describes the electromagnet force applied on the ball based on the Newton's 2nd law:

$$F_{ac} = F_{gf} - F_{em} \quad (3)$$

Where:

F_{ac} = The acceleration Force of the magnetic ball

F_{em} = The electromagnetic attraction Force for the magnetic ball

F_{gf} = The gravity Force of the magnetic ball

The dynamic behaviour of the electromagnetic force is described by nonlinear behaviour of Eq. 4 (Baranowski and Piatek, 2012; Muresan *et al.*, 2015; Antic *et al.*, 2013):

$$F_{em} = k_{mf} \left(\frac{i}{y} \right)^2 \quad (4)$$

Where:

k_{mf} = The magnetic force constant

y = The ball position

Therefore, the mathematical model of the second part can be described by Eq. 5 after substituting Eq. 2 in Eq. 4 which represents the open-loop nonlinear and unstable system:

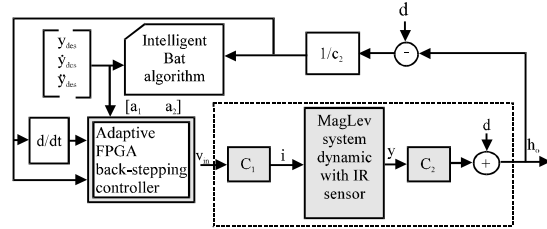


Fig. 2: The proposed controller structure

$$\ddot{y}m = mg - k_{mf} \left(\frac{C_1 \times v_{in}}{y} \right)^2 \quad (5)$$

Where:

m = The ball mass

g = The gravitation constant value which equals 9.81 (msec⁻²)

\dot{y} = The ball velocity

\ddot{y} = The ball acceleration

Adaptive intelligent FPGA back-stepping controller design:

The main task of the proposed an adaptive intelligent FPGA-back-stepping controller is to generate an adaptive voltage control action that controls the electromagnetic current where the attraction force acting on the steel ball by adjusting the electromagnetic force until it equals the gravitational pull appearing on it and achieving the desired position of the ball in the magnetic field and stabilizing it. The general structure of the proposed controller is shown in Fig. 2. There are three steps towards designing the proposed controller:

First step: In this step, the back stepping control law is derived as follows: the tracking position error of the magnetic ball is defined as in Eq. 6:

$$x_1 = y - y_{des} \quad (6)$$

where, y_{des} is the desired ball position. The first derivation for Eq. 6 is written as in Eq. 7:

$$\dot{x}_1 = \dot{y} - \dot{y}_{des} \quad (7)$$

The stability function is defined as in Eq. 8:

$$\lambda = -a_1 x_1 + \dot{y}_{des} \quad (8)$$

where, a_1 is the adaptive positive value. The velocity of the magnetic ball is defined as in Eq. 9:

$$x_2 = \dot{y} - \lambda \quad (9)$$

The acceleration of the magnetic ball is defined in Eq. 10 by taking the first derivative of Eq. 9:

$$\dot{x}_2 = \ddot{y} - \dot{\lambda} \tag{10}$$

Where:

$$\dot{\lambda} = -a_1 \dot{x}_1 + \ddot{y}_{des} \tag{11}$$

Then, Eq. 10 becomes Eq. 12 after substituting in Eq. 11:

$$\dot{x}_2 = \ddot{y} + a_1 \dot{x}_1 + \ddot{y}_{des} \tag{12}$$

Then substituting Eq. 5 into Eq. 12 gives Eq. 13:

$$\dot{x}_2 = g - \frac{k_{mf}}{m} \frac{(C_1 v_{in})^2}{y^2} + a_1 \dot{x}_1 + \ddot{y}_{des} \tag{13}$$

To confirm that the closed loop control law for the nonlinear MagLev system is asymptotically stable, Lyapunov criterion is used as follows (Izadi and Dubljevic, 2015):

$$V = 0.5x_1^2 + 0.5x_2^2 \tag{14}$$

The time derivative of Eq. 14 is taken to give Eq. 15:

$$\dot{V} = x_1 \dot{x}_1 + x_2 \dot{x}_2 \tag{15}$$

Then substituting Eq. 7 and 8 in Eq. 15 gives Eq. 16:

$$\dot{V} = -a_1 x_1^2 + x_1 x_2 + x_2 \dot{x}_2 \tag{16}$$

Putting Eq. 16 in asymptotically stable form yields Eq. 17:

$$\dot{V} = -a_1 x_1^2 - a_2 x_2^2 \leq 0 \tag{17}$$

where, a_2 is the adaptive positive value. Substituting Eq. 13 into Eq. 16 leads to Eq. 18:

$$\dot{V} = -a_1 x_1^2 + x_1 x_2 + x_2 \left(g - \frac{k_{mf}}{m} \frac{(C_1 v_{in})^2}{y^2} + a_1 \dot{x}_1 - \ddot{y}_{des} \right) \tag{18}$$

Finally, the control law that makes the system operation asymptotically stable is given by the following Eq. 19:

$$v_{in} = \sqrt{\frac{m}{k_{mf} C_1} y^2 (x_1 + a_1 \dot{x}_1 + a_2 x_2 + g - \ddot{y}_{des})} \tag{19}$$

It is clear that when x_1 and x_2 are equal to zero, V and \dot{V} are also equal to zero. But when x_1 and x_2 are not equal to

zero, V is a positive (not equal to zero) value while \dot{V} is a negative (not equal to zero) value. This means that the closed loop feedback control of MagLev system is asymptotically stable in all regions of operation. Finally, the control gain parameters a_1 and a_2 are tuned and obtained using the IBO algorithm in order to speed up the transient state of the control action that leads to reach the magnetic ball in the desired position fast with minimum error without over shoot and with no oscillation in the output response.

Second step: This step explains the use of Intelligent Bat Optimization Algorithm (IBOA) for tuning and obtaining the best control parameters a_1 and a_2 of the controller in order to provide an improved solution and to obtain high-speed in the real-time application for the controller performance in terms of generating fast and optimal control action through finding and tuning the control parameters a_1 and a_2 of the back-stepping control law equation that will lead to reduce the position error of the magnetic ball and reach to the desired position.

MATERIALS AND METHODS

The proposed procedure is summarized by the following points: Define the objective function $f(x_i)$ and fitness function Eq. 20 and 21, respectively. The mean square error is used in order to evaluate the performance of the control system as in Eq. 20:

$$f(x_i) = PI(i) = \frac{1}{N} \sum_{i=1}^N [(y_{des} - y)^2 + (\dot{y}_{des} - \dot{y})^2 + (\ddot{y}_{des} - \ddot{y})^2] \tag{20}$$

The fitness function is calculated by using Eq. 21 based on the performance index in Eq. 20:

$$fitness = \frac{1}{\mu + PI} \tag{21}$$

where, $\mu > 0$ to avoid division by zero. Initialize the bat populations x_i and velocity v_i , here population size $i = 32$ the number of iterations $N = 20$. Initialize the pulse frequency f_i for each bat which is generated randomly between $f_{min} = 0$ and $f_{max} = 2$. Initialized the pulse rate r_i and loudness A_i randomly such as $r_i \in [0,1]$ and $A_i \in [1, 2]$ (Yang, 2010):

- Find the best current solution (x_*)
- Start the loop { ($t < N$)
- Generate new solutions by adjusting pulse frequency and update velocity and location by using the following Algorithm 1.

Algorithm 1; IBOA algorithm:

$f_i = f_{min} + (f_{max} - f_{min})\beta$ where, $\beta \in (0, 1)$ random vector from a uniform distribution (Yang, 2010):

$$v_i^1 = v_i^{t-1} + v_i^1(x_i^t - x_*)f_i$$

$$x_i^1 = x_i^{t-1} + v_i^1$$

Make a condition (rand > r_i). Yes{select a solution among the best solutions and generate a local solutions around the selected best. Solution $x_{new} = x_{old} + \epsilon A^1$ where $\epsilon \in [-1, 1]$ is a random vector from a uniform distribution
}

No{end condition}

- Generate a new solution by flying randomly as follows:

Make the condition (rand < A_i and f(x_i) < f(x*))

Yes{Accept the new solution

Increase r_i and decrease A_i}

No {end the condition}

- Rank the bats and find the current best x*
- Plot the results

The above procedure is repeated every 0.005 sec for each kth sample based on Shannon theorem. To implement the on-line (IBOA) which is used to obtain and tune the control parameters.

Third step: The schematic design of the adaptive FPGA-back-stepping controller is implemented by using the Xilinx development tool with ISE Ver. 14.5. Here, the continuous equation of the proposed control law is replaced by a digital equation based on the bilinear z-transform as in Eq. 22:

$$u(z) = \sqrt{\frac{m}{C_1^2 k_{mf}} y^2(z) [y(z) - y_{des} + a_1 \frac{1-z^{-1}}{T_s} y(z) - a_1 \dot{y}_{des} + a_2 \left(\frac{1-z^{-1}}{T_s} y(z) - \dot{y}_{des} \right) + a_2 a_1 (y(z) - y_{des}) + g - \ddot{y}_{des}]}{22}}$$

where, T_s is the sampling time. Then by converting from z-transform to discrete time at kth samples, the voltage control action u(k) becomes as follows:

$$u(k) = \sqrt{\frac{m}{C_1^2 k_{mf}} y^2(k) [y(k) - y_{des} + \frac{a_1}{T_s} [y(k) - y(k-1)] - a_1 \dot{y}_{des} + \frac{a_1}{T_s} [y(k) - y(k-1)] - a_2 \dot{y}_{des} + a_2 a_1 (y(k) - y_{des}) + g - \ddot{y}_{des}]}{23}}$$

Based on Eq. 23 and by converting it to Eq. 24 as simple equation, the structure of the FPGA-back-stepping controller is demonstrated in the block diagram of Fig. 2:

Table 2: The control signals of the digital 2's complement circuit

No. of clock	CS in	CS CO	CS out	Output
Two	1	0	0	0
Two	0	1	0	0
Two	0	0	1	Out

$$u(k) = \sqrt{\frac{m}{C_1^2 k_{mf}} y(k) \left[(y(k) - y_{des}) \times (1 + a_2 a_1) + (y(k) - y(k-1)) \times \left(\frac{a_1}{T_s} + \frac{a_2}{T_s} \right) + g \right]}{24}}$$

Assume \dot{y}_{des} and \ddot{y}_{des} are equal to zero, therefore, the constraint of the proposed control law can be seen in Eq. 25 in order to design and implement it and to avoid the numerical errors:

$$\left| (y(k) - y_{des}) \times (1 + a_2 a_1) + (y(k) - y(k-1)) \times \left(\frac{a_1}{T_s} + \frac{a_2}{T_s} \right) \right| \leq g \quad (25)$$

The finite word length is decided in the digital back-stepping controller design as eighteen bits (Williamson, 1991; Khedker and Khade, 2017). One bit for sign, seven bits for integer and ten bit for fraction for all registers, adder/subtractor, multiplier and square root ICs. The block diagram of the proposed controller can be observed in Fig. 3. The schematic design of digital back-stepping controller consists of three modules as follows:

Two's complement arithmetic module: The two's complement module is very important in the digital Back-stepping controller to deals with signed numbers efficiently. The description of FPGA two's complement components design are: four registers ICs 18-bits, one adder IC 18-bit and 18 multiplexers ICs with some logic gates as shown in Fig. 4a, b. Then using high level Verilog programming language to test the operation of the two's complement module as shown in Fig. 4c. Table 2 shows the control signals of the digital circuit. The design of the digital 2's complement needs the following: (294) slices LUTs, (290) logic gate, (180) occupied slices, (290) LUT flip-flop pairs, (164) flip-flop and (41) bonded IOBs.

Adaptive back-stepping control law module: The adaptive back-stepping control law defined in Eq. 25 is designed as shown in Fig. 3 with the following ICs requirements: 12 register ICs, 6 adder/subtract ICs, 5 multiplier ICs and 1 square-root IC as shown in Fig. 5a, b with the following component numbers: (482) slices LUTs, (481) logic gate, (320) occupied slices, (481) LUT flip-flop pairs,

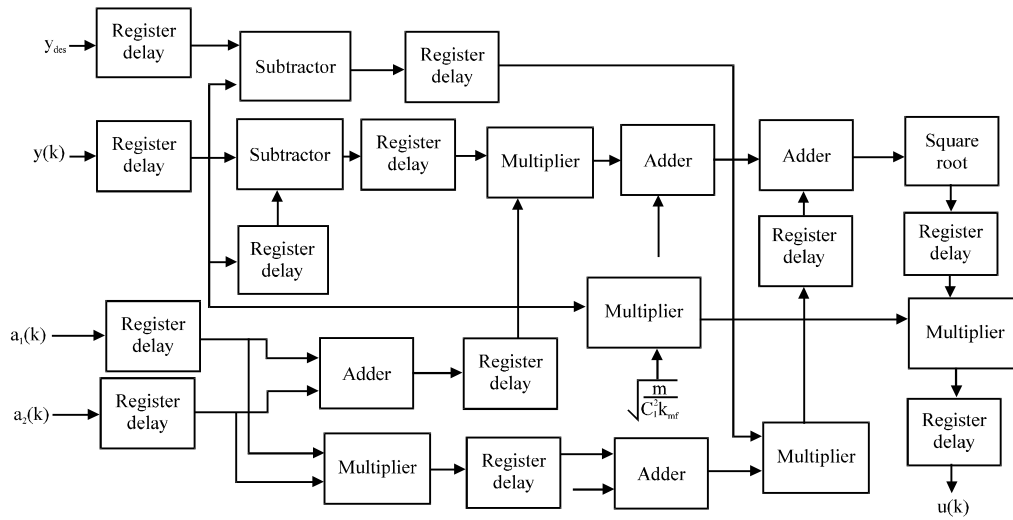


Fig. 3: The block diagram of the adaptive intelligent FPGA back-stepping controller design

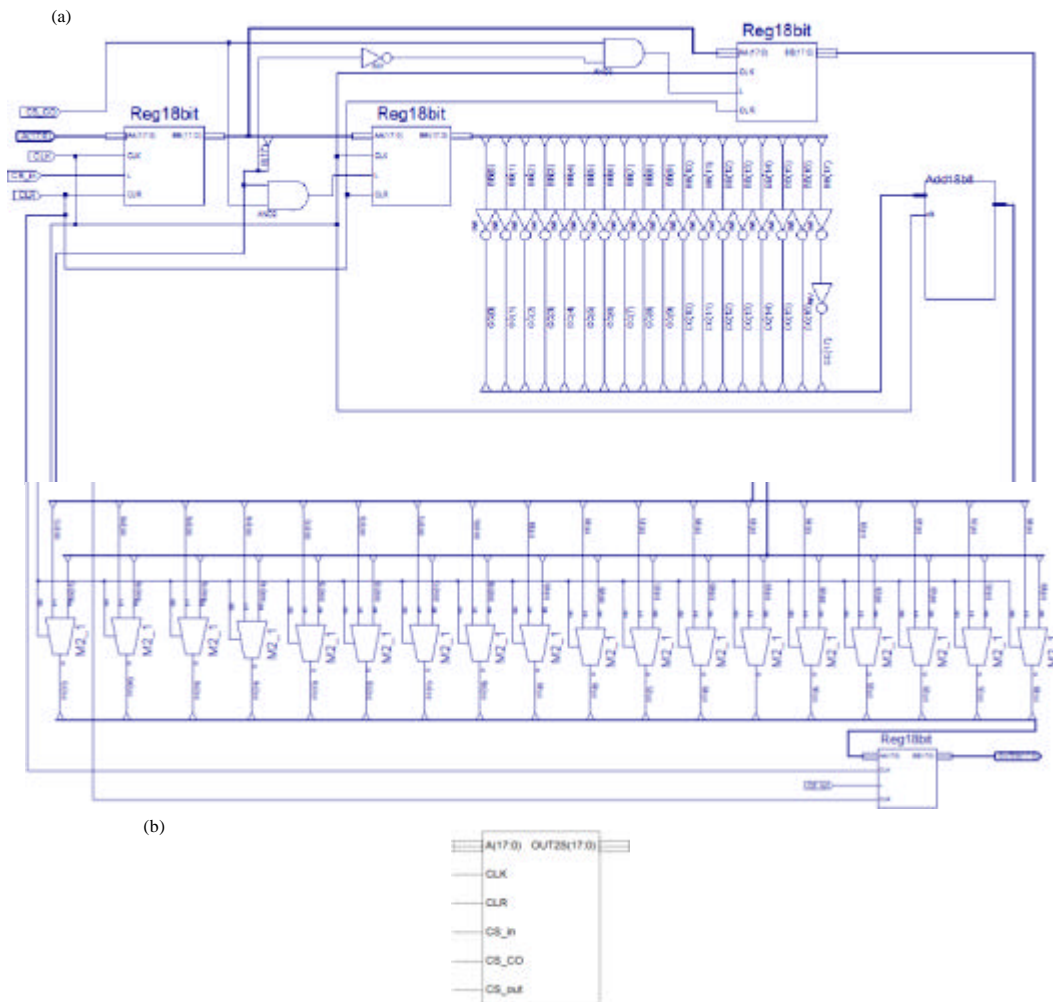


Fig. 4: Continue



Fig. 4: Digital circuit of the 2's complement arithmetic: a) Schematic design; b) Top level design and c) Waveform of the operation

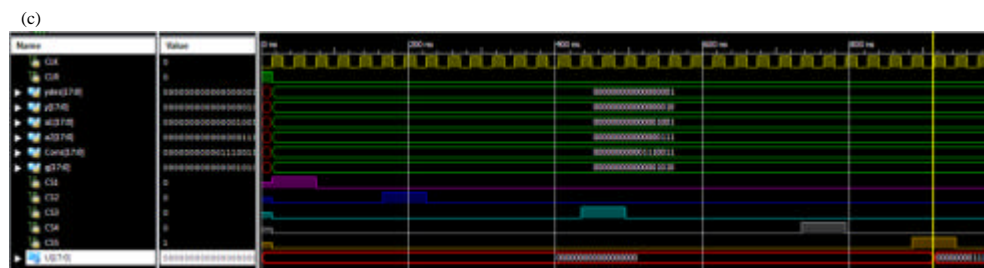
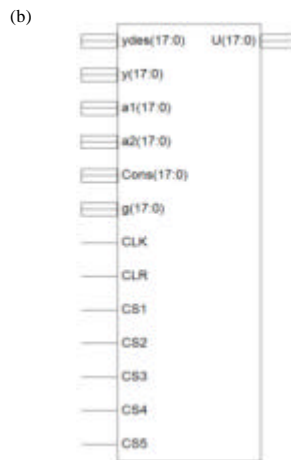
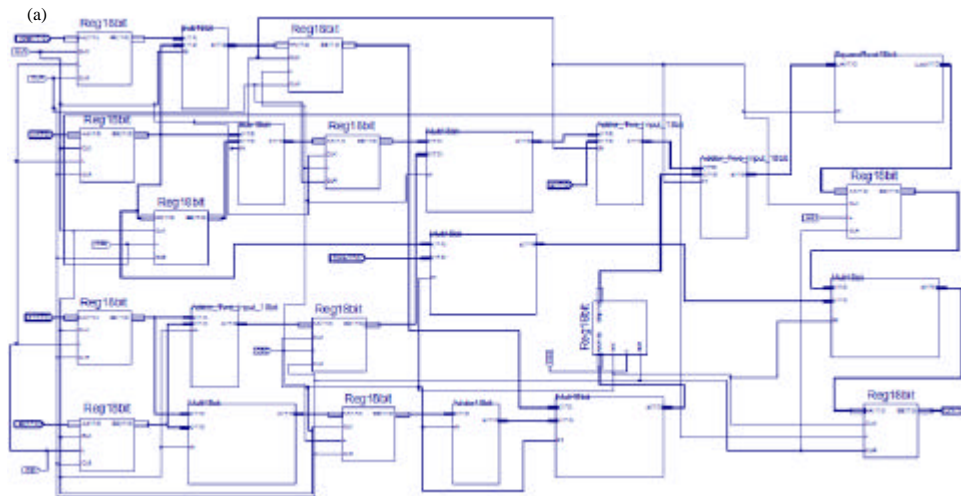


Fig. 5: Adaptive digital back-stepping circuit of control law: a) Schematic diagram; b) Top level design and c) The diagram of control signals

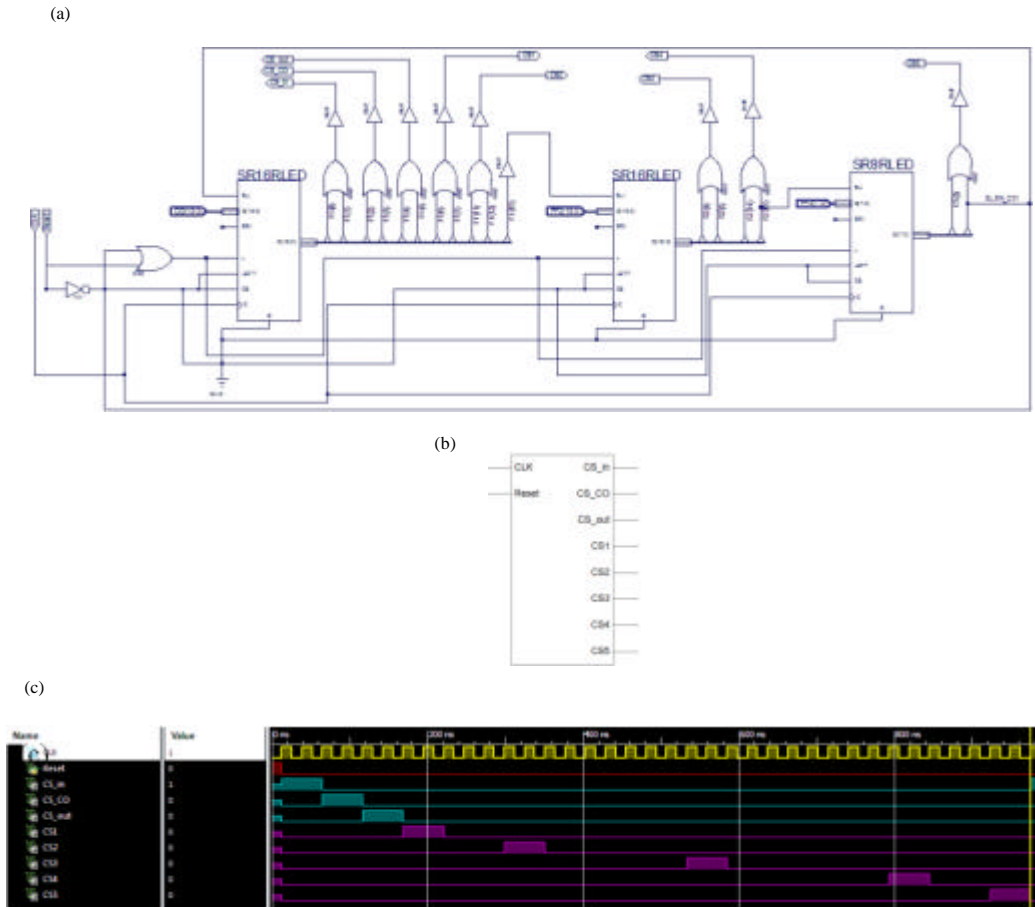


Fig. 6: Control unit circuit: a) Digital schematic diagram; b) Top level design diagram and c) The test bench control waveform signals

(322) flip-flop and (131) bonded IOBs. The operation of this module can be described in Fig. 5c based on Verilog language with five control signals needed to operate the digital control law as shown in Table 3.

Digital control module design: To investigate the operation of the adaptive intelligent FPGA back-stepping controller, there is a need to synchronize and control the data flow in the two's complement arithmetic module and back-stepping control law module. This can be achieved by designing a 37-bits shift-register digital control module by using two 16-bits shift-register and one 8-bits shift-register through serial connection for generating a sequence of pulses as shown in Fig. 6a, b. The frequency of each pulse is equal to 7.4 kHz in order to achieve the sampling time of the MagLev system which is equal to 0.005 sec during 37 clocks or pulses.

Then the Verilog language is used for simulating the control module as shown in Fig. 6c. The components of the schematic design of the digital control module need

Table 3: The control signals of the adaptive digital back-stepping control law

No. of clock	CS1	CS2	CS3	CS4	CS5	Action
Two	1	0	0	0	0	X
Three	Delay for adder/subtractor and multiplier parallel operations					X
Two	0	1	0	0	0	X
Seven	Delay for two adders and three multipliers serial operations					X
Two	0	0	1	0	0	X
Eight	Delay for adder and square root serial operations					X
Two	0	0	0	1	0	X
Three	Delay for multiplier operation					X
Two	0	0	0	0	1	Action

the following: (162) slices LUTs, (165) logic gate, (180) occupied slices, (165) LUT flip-flop pairs, (84) flip-flop and (10) bonded IOBs.

Finally, Fig. 7a, b show the adaptive FPGA back-stepping controller IC as the overall design and the top level schematic diagram with its pins and control signals, respectively. The inputs to the FPGA

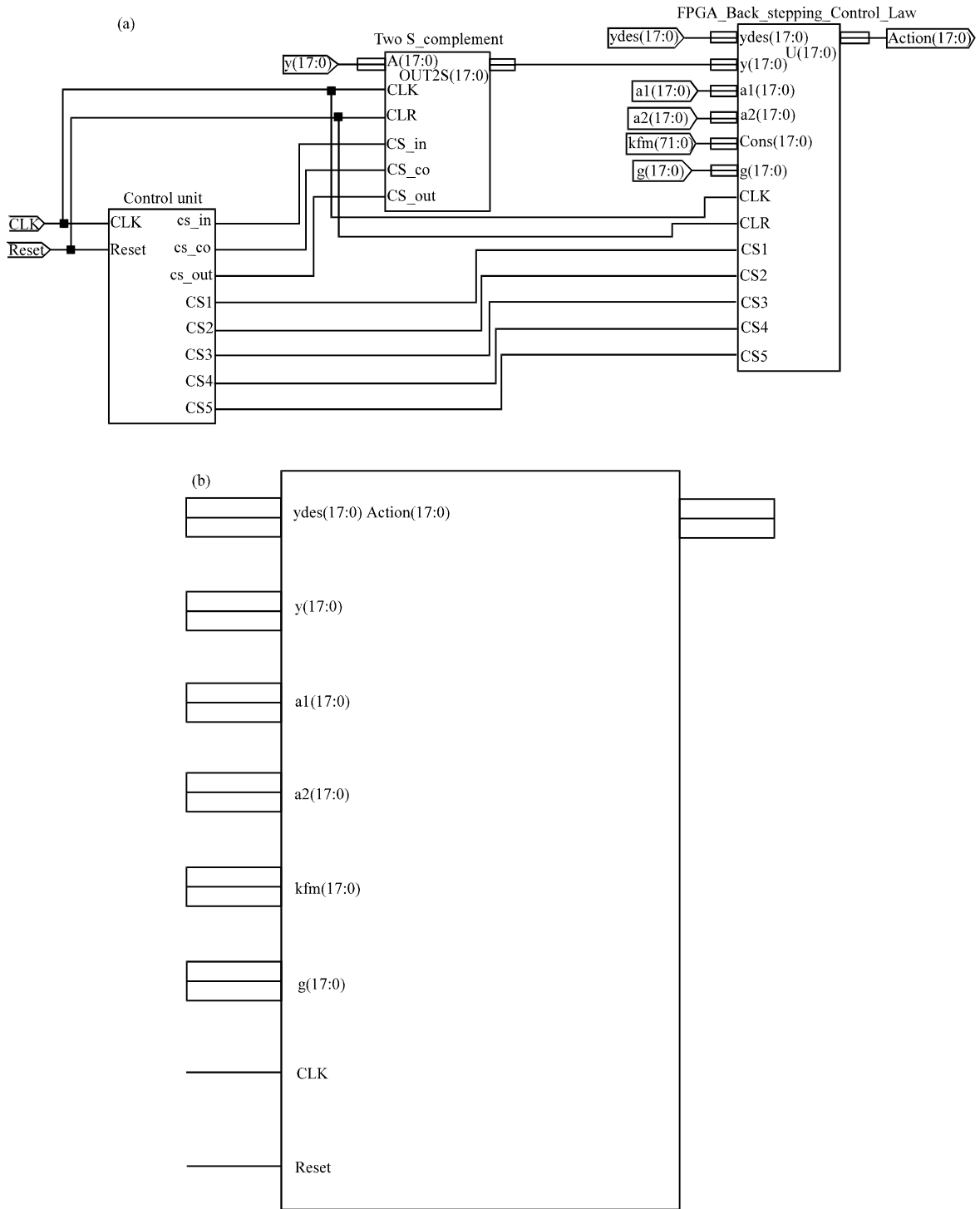


Fig. 7: a) The adaptive FPGA back-stepping controller and b) The top level diagram of adaptive FPGA back-stepping controller IC

back-stepping controller are: y_{des} , y , a_1 , a_2 , $\sqrt{m/(C_1^2 k_{mf})}$, g reset and clock generator. The overall components of the FPGA-back-stepping controller are as follows: (938)

slices LUTs, (936) logic gate, (680) occupied slices, (951) LUT flip-flop pairs, (570) flip-flop and (128) bounded IOBs.

RESULTS AND DISCUSSION

Numerical simulation results and experimental work:

The MagLev 33-201 feedback instrument model is shown in Fig. 8 which is considered as one of the educational devices for teaching control of nonlinear system dynamics. The measured position is determined from an array of infrared transmitters and detectors, positioned in such a way that the infrared beam is intersected by the sphere. The infrared photo sensor is assumed to be linear in the required range of operation.

To apply the proposed structure of the controller on MagLev system, MATLAB package is used. The numerical simulation is done by applying the 4th order Runge Kutta method with 0.005 sec sampling time.

Figure 9 shows the open loop response for the position of the magnetic ball in the MagLev system which has a very fast and unstable response due to the strong nonlinear dynamic behavior of the system that is to say the magnetic steel ball is rapidly falling or attracting to the electromagnetic pole of the MagLev system. Therefore, the back stepping controller is very essential to stabilize the position of steel ball accurately in the desired position suspended inside the magnetic field.

The numerical simulation results for the MagLev variable steel ball position with on-line tuning closed loop feedback adaptive back-stepping control system are shown in Fig. 10a-c. The desired magnetic ball position is taken from Qin *et al.* (2014) as the variable step position change of (-1.5, -2, -1, -2 and -1) volt in order to compare with two types of the controllers that described by Qin *et al.* (2014) and to show the effectiveness of the proposed controller in terms of a fast response without any overshoots and it has a zero steady-state the error value at each step position as shown in Fig. 10a.

Figure 10b shows the steel ball position error between the desired position (y_{des}) and the actual position (y). It has a very small value in the transient region and reaches zero in the steady state region.

Figure 10c shows the adaptive performance of the proposed an adaptive intelligent controller based on the back-stepping method has a fast and smooth control action with small spikes and no oscillations as well as no saturation state. Moreover, this control action has the ability to deliver a stable suspension of the steel ball in the desired position.

To confirm that the closed loop feedback adaptive intelligent back-stepping controller for the MagLev system is stable during 1500 samples, the phase-plane plot is used to illustrate the relationship between the



Fig. 8: Magnetic levitation feedback 33-201 model

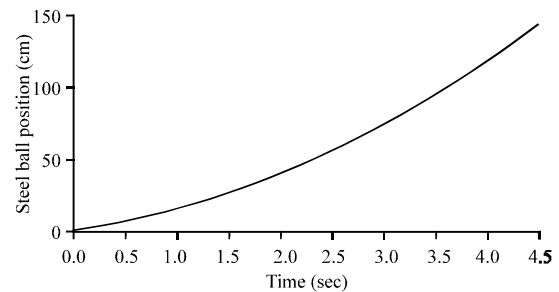


Fig. 9: Steel ball position in open loop response for MagLev system

position and velocity of the steel ball as shown in Fig. 11. The performance of the adaptive intelligent back-stepping controller with the on-line tuning algorithm has obviously in the improved position response of the steel ball and this can be seen from the error convergence for the MagLev system which was based on the proposed mean square error function as defined by Eq. 20 during the carried out 1500 samples as shown in Fig. 12.

Figure 13 shows the on-line adaptation of the parameters of the adaptive intelligent back-stepping controller a_1 and a_2 in order to speed up the transient response of the closed loop control system that depends on the initial parameters of the IBO algorithm.

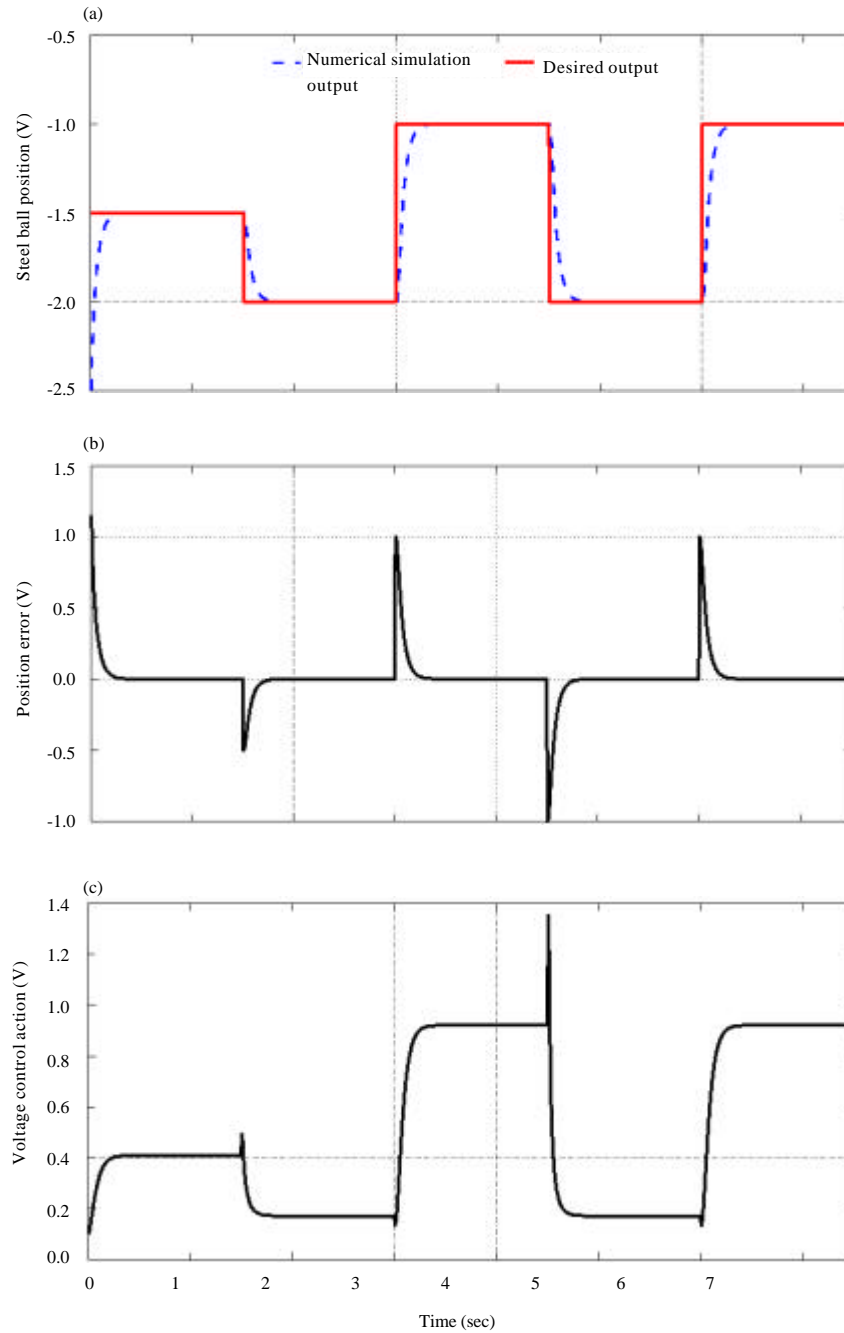


Fig. 10: Numerical simulation results: a) Steel ball position output; b) Position error and c) Voltage action

Also, to confirm the online tuning control parameters of the adaptive back-stepping control system has high effectiveness in terms of the steel ball reached the desired position faster with high reduction in the position tracking error and smooth voltage control action which is generated with very small spikes and no saturation state. The desired magnetic ball position is taken from Pati *et al.* (2016) as the square step

change of (-1.1 to -1.5) V in order to compare with the controller that proposed by Pati *et al.* (2016).

Figure 14a shows a fast excellent response of the magnetic ball without any overshoots and it has a zero steady-state the error value at each step position. Figure 14b shows the performance of the proposed controller which has a fast and smooth control action with small spikes and no saturation state.

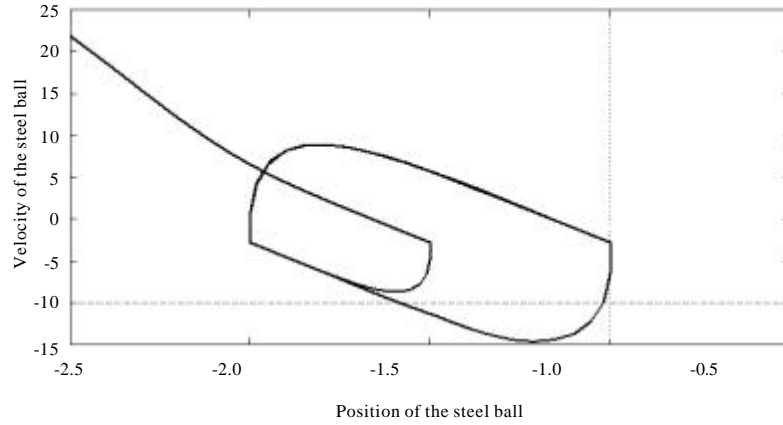


Fig. 11: The relation-ship between the steel ball positions against its velocity

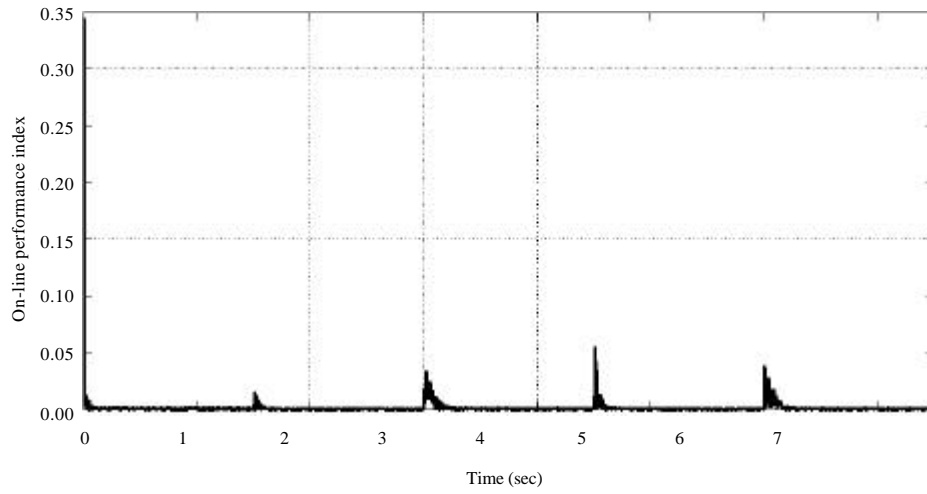


Fig. 12: Online performance index

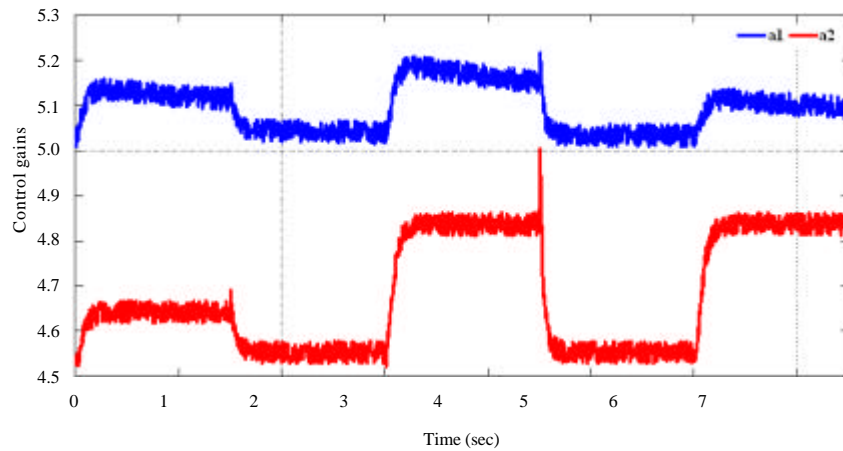


Fig. 13: The adaptive control parameters of the controller during 1500 samples

Two different models of the MagLev models are taken from Al-Araji (2016) and Abu Elreesh and Hamed (2012) in order to investigate the effective performance of the proposed adaptive control algorithm in terms of high

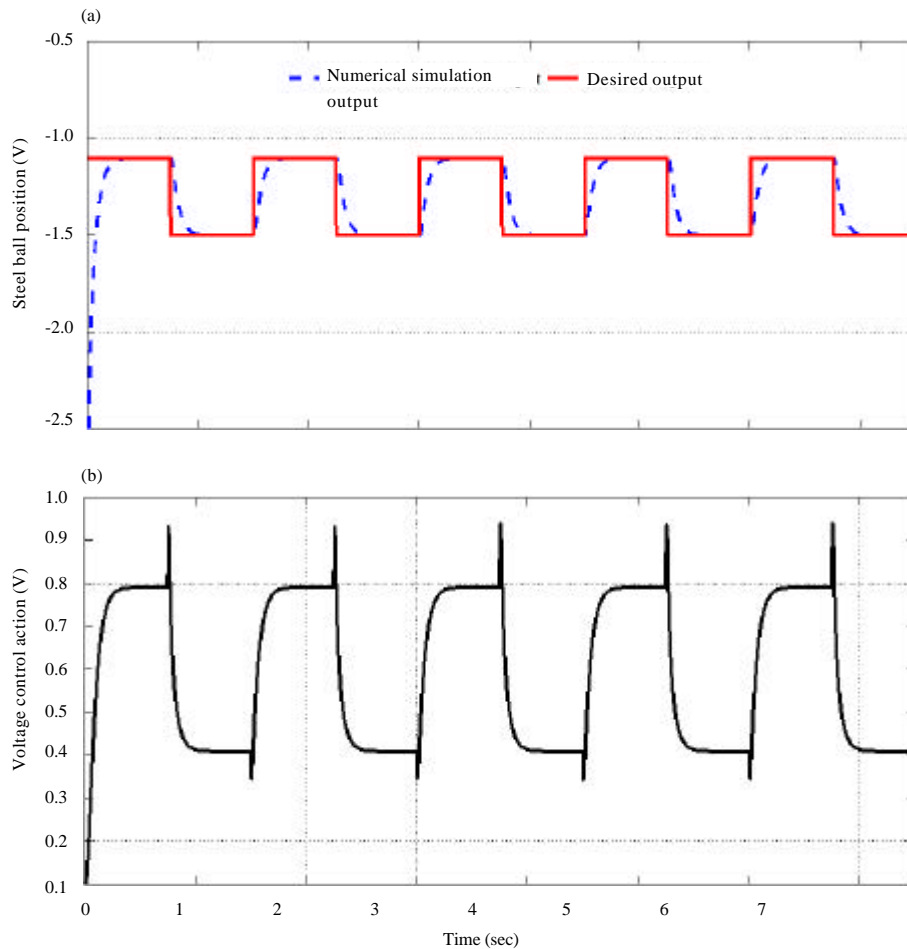


Fig. 14: Numerical simulation results: a) Steel ball position output and b) Controller output

Table 4: The physical parameters (Al-Araji, 2016)

Parameters	Values
Control input voltage level (v_m)	-5 to 5 V
Magnetic ball mass (m)	0.0413 kg
Constant of magnetic force (k_m)	$\text{kg}\cdot\text{m}^3/\text{s}^2/\text{A}^2$
Coil resistance (R)	1.71 Ω
Coil inductance (L)	15.1 mH
Hall effect sensor constant (α)	2.48 V
Γ	0.31 V/A
B	4.25×10^4

computational control parameters accuracy and minimizing the magnetic ball position error and obtaining smooth voltage action without sharp spikes.

The first model is hall effect sensor MagLev that is taken from Al-Araji (2016) and the physical parameters illustrated in Table 4 (Al-Araji, 2016).

The set point is unit step has value 2 cm which is the equilibrium point of the hall effect sensor MagLev Model. Figure 15 shows the steel ball position of the MagLev which is very fast and smooth response with the time specifications of 0.133 sec settling time 0.091 sec rising time and no overshoot at transient state. At steady-state

the steel ball position approaches to zero radian when it compared with a nonlinear controller which is taken from (Al-Araji, 2016) as shown in Table 5. The second model is MagLev CE152 that is taken from (Abu Elreesh and Hamed, 2012) and the physical parameters illustrated in Table 6.

The set point is unit step has value 0.5 cm which is the equilibrium point of the MagLev Model CE152. Figure 16 shows the steel ball position of the MagLev which is very fast and smooth response with the time specifications of 0.14 sec settling time 0.093 sec rising time and no overshoot at transient state. At steady-state the steel ball position approaches to zero radian when it compared with a nonlinear controller which is taken from (Abu Elreesh and Hamed, 2012) as shown in Table 7.

The Xilinx Virtex5xc5v1x50 Kit is used as shown in Fig. 17a in order to verify the proposed schematic design of the adaptive FPGA back-stepping controller as shown in Fig. 17 for a real-time MagLev system, we will use the sequence of operations for Xilinx-ISE Version 14.5 as (synthesize-XST, implement design and generate

programming file) then generate the bit-stream file for the proposed controller and download the bit-stream file to the Xilinx Virtex5xc5vlx50 Kit as shown in Fig. 17b. Then, the Xilinx Virtex5xc5vlx50 Kit is connected externally as a hardware controller to the real MagLev system with the

utilization of the NI-DAQmx-USB 6009 device which is connected to the PC (Laptop) through the USB cable as a data acquisition system. The overall experimental hardware setup in real-time controller for the MagLev system is shown in Fig. 18.

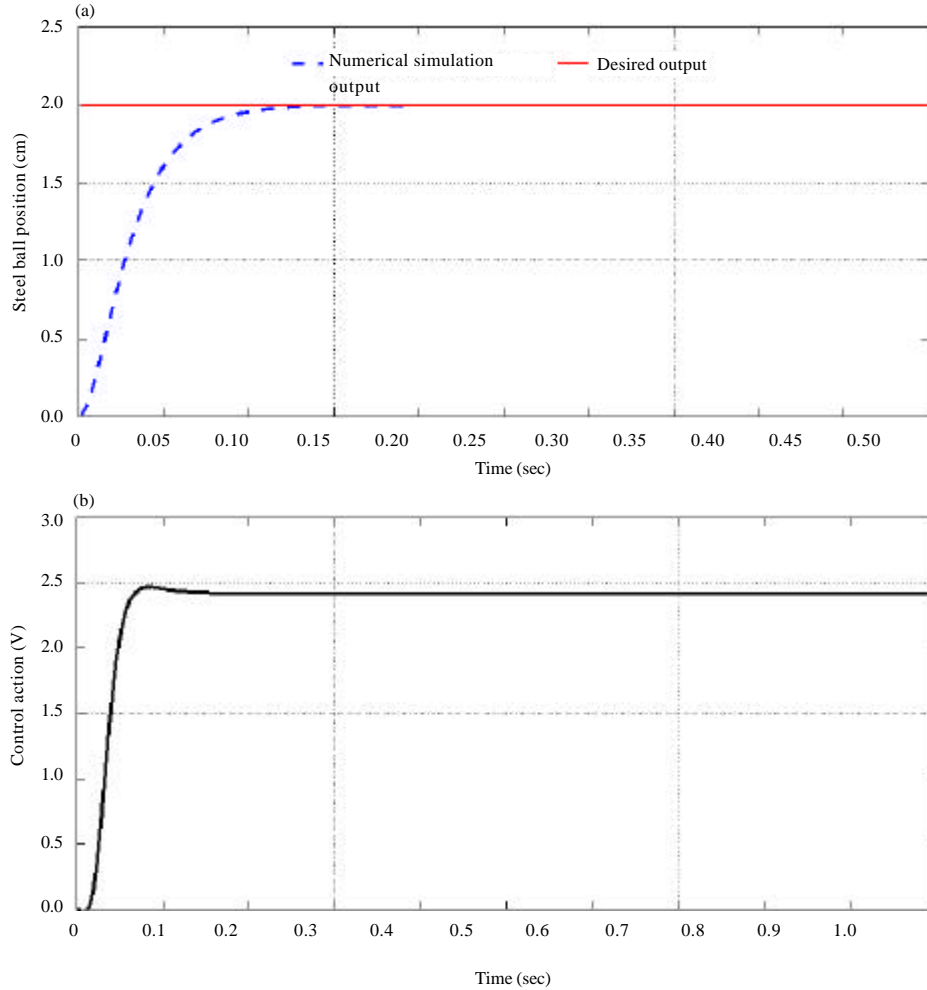


Fig. 15: Numerical simulation results based on the parameter values of the MagLev Model by Al-Araji (2016): a) Steel ball position output and b) Controller output

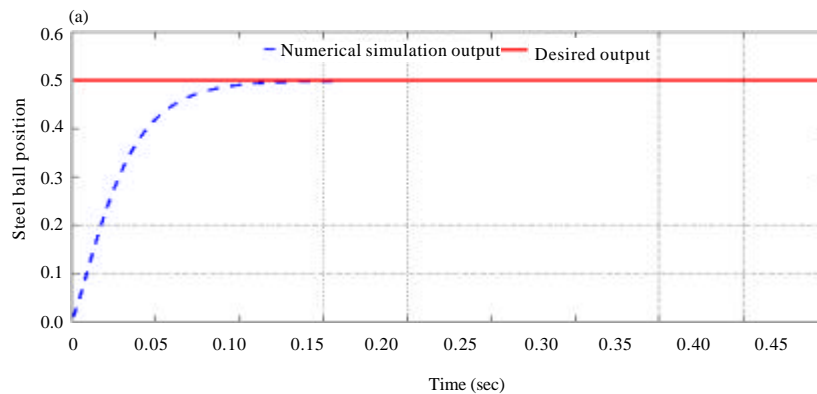


Fig. 16: Continue

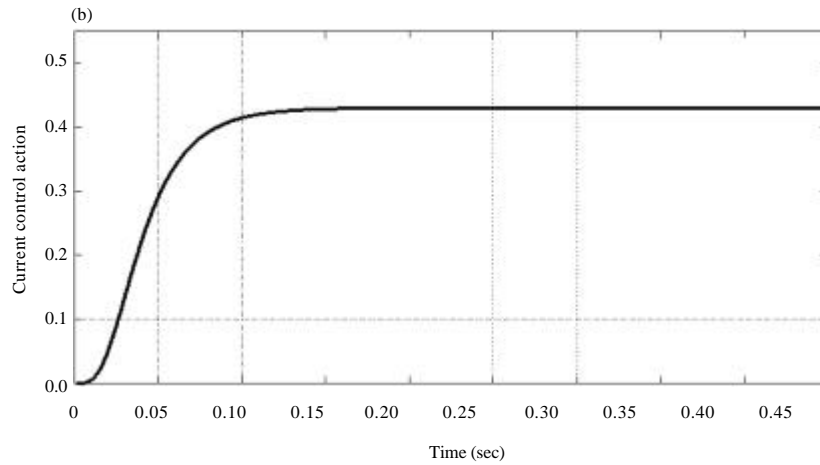


Fig. 16: Numerical simulation results based on the parameter values of the MagLev Model by Abu Elreesh and Hamed (2012): a) Steel ball position output and b) Controller output

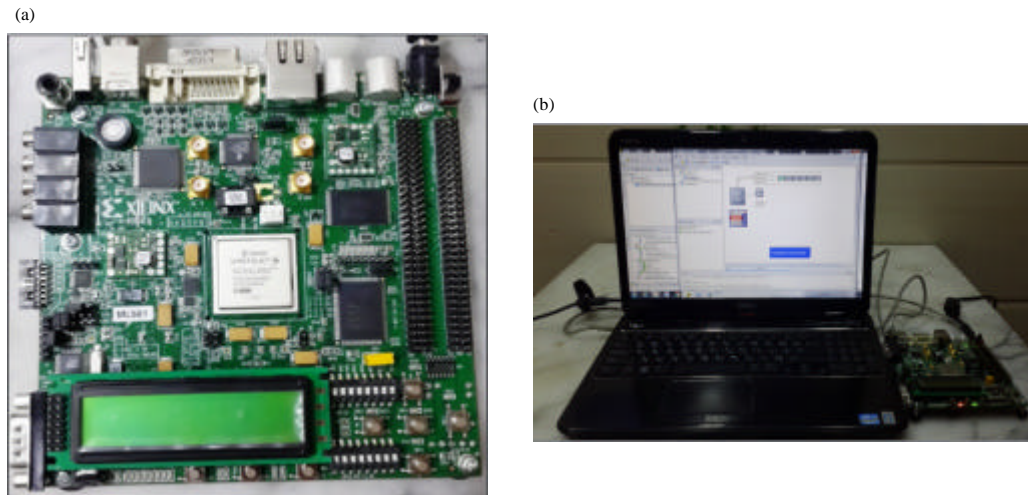


Fig. 17: a) The Xilinx Virtex5 xc5vlx50 Kit and b) Generating and downloading the bit-stream file to the kit

Table 5: The steel ball tracking performance comparison between the proposed controller and the controller by Al-Araji (2016)

Types of controller	Settling time (sec)	Rising time (sec)	Steady-state error	Overshoot (%)	No. of iterations
Proposed controller	0.133	0.091	0.0	0.00	20
Cognitive nonlinear controller (Al-Araji, 2016)	0.480	0.360	0.0	5.38	100

Table 6: The physical parameters (Abu Elreesh and Hamed, 2012)

Parameters	Values
Magnetic ball mass (m)	0.00837 (kg)
Constant of coil (Kc)	8.0915×10^6 (N.m ² A ⁻²)
Damping constant (k _v)	0.0195 (N.s.m ⁻¹)
Coil offset (x ₀)	0.0083 (m)

Table 7: The steel ball tracking performance comparison between the proposed controller and the controller by Abu Elreesh and Hamed (2012)

Types of controller	Settling time (sec)	Rising time (sec)	Steady-state error	Overshoot (%)
Proposed controller	0.14	0.098	0.0	0.0
Fuzzy controller (Abu Elreesh and Hamed, 2012)	0.20	0.106	0.0	0.0

LabVIEW 2014 package is used for monitoring the experimental results as shown in Fig. 19a-d which confirm

the performance of the adaptive FPGA back-stepping controller for the real-time magnetic levitation system with

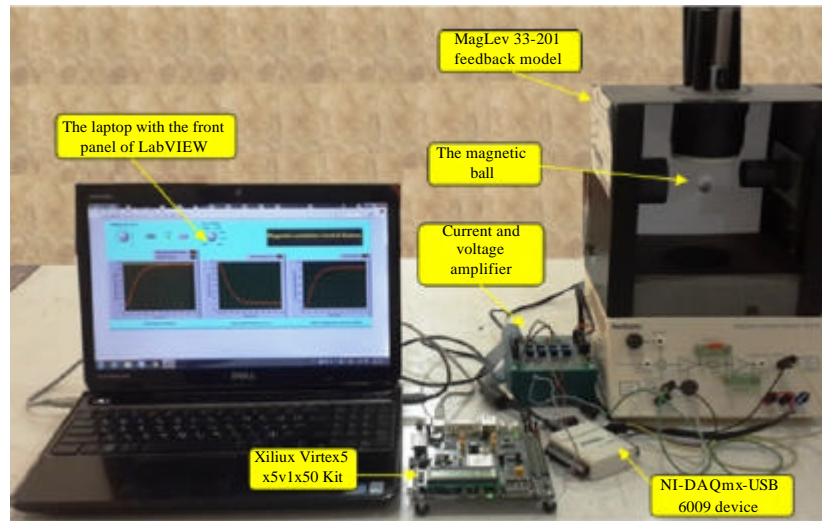


Fig. 18: The experimental hardware setup in real-time system

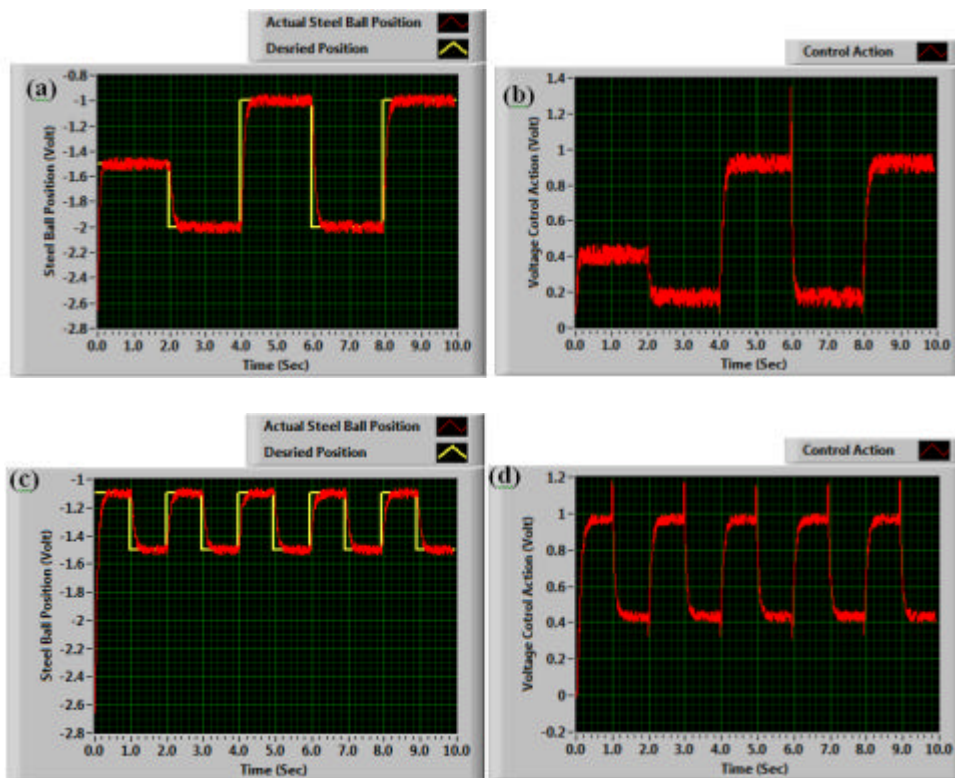


Fig. 19: Real-time adaptive FPGA back-stepping controller results: a) Actual steel ball position case 1; b) Voltage action case 1; c) Actual steel ball position case 2 and d) Voltage action case 2

the MATLAB simulation results. Figure 19a, c show the actual steel ball position in case 1 and 2 which represents the voltage of the system based on the measured voltage

of the IR sensor by using the first channel ADC for NI-DAQmx-USB 6009 device. The desired position of the magnetic ball is taken from Fig. 10a and 14a for case

1 and 2, respectively. The steel ball position response delivered by the proposed system exhibited fast response in transit-state without any overshoots and only small output oscillation in the steady-state can be observed, this oscillation is due to several parameters affecting the measurement process such as noise effect, the external bounded disturbance and the uncertain system parameters variations which have a highly nonlinear dynamic behaviour. Figure 19b, d illustrates the performance effect of the voltage control action of digital back-stepping controller on steel ball position in the magnetic field in terms of fast reaching and maintaining the steel ball in the desired position without any overshoots in the control action along with minute oscillation in steady-state. The second channel of the NI-DAQmx-USB 6009 ADC input was used to read the control action signal.

There are small differences between the simulation and the real time results because of several reasons such as: hardware error as the offset and the nonlinearity equation in the IR sensor, noise effect of the operational amplifiers, the external bounded disturbance and the data converter quantization error. It is important to mention that the developed system of the Xilinx Virtex5 Kit depends on the proposed finite word length which was 18 bits, therefore, there is a small oscillation error in the real-time result of the steel ball desired position for MagLev system.

CONCLUSION

In this research, the adaptive intelligent FPGA back-stepping nonlinear controller based on Lyapunov criterion with intelligent bat optimization tuning algorithm for MagLev system has been designed and simulated for different desired positions using MATLAB package. The FPGA Virtex5xc5v1x50 Kit with ISE for Xilinx development tool has been used to make the schematic design, simulate and verify the adaptive intelligent FPGA back-stepping nonlinear controller in the real-time MagLev system after converting the proposed adaptive continuous control law equation to the proposed adaptive digital control law equation. From the numerical simulation and experimental results, the performance of the proposed an adaptive intelligent continuous and adaptive intelligent digital controllers proved that:

- The steel ball reached the desired position faster with exceptionally slight oscillation
- High reduction in the steel ball position tracking error index that reaches approximately zero value

- Smooth voltage control action which was generated without spikes and no saturation state, so as to track the desired steel ball position with high precision

Because a newly designed on-line auto-tuning structure is presented for the adjustment of the control gains and the stability analysis of the designed controller is realized via. Lyapunov method.

REFERENCES

- Abu Elreesh, H. and B. Hamed, 2012. FPGA fuzzy controller design for magnetic ball levitation. *Int. J. Intell. Syst. Applic.*, 4: 72-81.
- Al-Araji, A.S., 2016. Cognitive non-linear controller design for magnetic levitation system. *Trans. Inst. Meas. Control*, 38: 215-222.
- Antic, D., M. Milovanovic, S. Nikolic, M. Milojkovic and S. Peric, 2013. Simulation model of magnetic levitation based on NARX neural networks. *Intl. J. Intell. Syst. Appl.*, 5: 25-32.
- Baranowski, J. and P. Piatek, 2012. Observer-based feedback for the magnetic levitation system. *Trans. Inst. Meas. Control*, 34: 422-435.
- Boonsatit, N. and C. Pukdeboon, 2016. Adaptive fast terminal sliding mode control of magnetic levitation system. *J. Control Autom. Electr. Syst.*, 27: 359-367.
- Ghosh, A., T.R. Krishnan, P. Tejaswy, A. Mandal and J.K. Pradhan *et al.*, 2014. Design and implementation of a 2-DOF PID compensation for magnetic levitation systems. *I SA. Trans.*, 53: 1216-1222.
- Iplikci, S. and B. Bahtiyar, 2016. A field-programmable gate array implementation of a real-time nonlinear Runge-Kutta model predictive control. *Trans. Inst. Meas. Control*, 38: 555-564.
- Izadi, M. and S. Dubljevic, 2015. Backstepping output-feedback control of moving boundary parabolic PDEs. *Eur. J. Control*, 21: 27-35.
- Javadi, A. and S. Pezeshki, 2013. A new model-free adaptive controller versus non-linear H8 controller for levitation of an electromagnetic system. *Trans. Inst. Meas. Control*, 35: 321-329.
- Khedkar, A.A. and R.H. Khade, 2017. High speed FPGA-based data acquisition system. *Microprocess. Microsys.*, 49: 87-94.
- Lin, F.J., L.T. Teng and P.H. Shieh, 2007. Intelligent adaptive backstepping control system for magnetic levitation apparatus. *IEEE. Trans. Magn.*, 43: 2009-2018.
- Muresan, C.I., C. Ionescu, S. Folea and R. De Keyser, 2015. Fractional order control of unstable processes: The magnetic levitation study case. *Nonlinear Dyn.*, 80: 1761-1772.

- Pati, A., V.C. Pal and R. Negi, 2016. Design of a 2-DOF control and disturbance estimator for a magnetic levitation system. *Eng. Technol. Appl. Sci. Res.*, 7: 1369-1376.
- Qin, Y., H. Peng, W. Ruan, J. Wu and J. Gao, 2014. A modeling and control approach to magnetic levitation system based on state-dependent ARX model. *J. Process Control*, 24: 93-112.
- Rubio, J.D.J., L. Zhang, E. Lughofer, P. Cruz and A. Alsaedi *et al.*, 2017. Modeling and control with neural networks for a magnetic levitation system. *DNeurocomputing*, 227: 113-121.
- Sadek, U., A. Sarjas, A. Chowdhury and R. Svecko, 2017. Improved adaptive fuzzy backstepping control of a magnetic levitation system based on symbiotic organism search. *Appl. Soft Comput.*, 56: 19-33.
- Trisanto, A., M. Yasser, J. Lu and T. Yahagi, 2006. Implementation of a fuzzy PID controller using neural network on the magnetic levitation system. *Proceedings of the 2006 International Symposium on Intelligent Signal Processing and Communications (ISPACS'06)*, December 12-15, 2006, IEEE, Tottori, Japan, ISBN:0-7803-9732-0, pp: 669-672.
- Williamson, D., 1991. *Digital Control and Implementation Finite Wordlength Consideration*. Prentice Hall, Upper Saddle River, New Jersey, USA., ISBN:9780132116404, Pages: 625.
- Yang, X.S., 2010. A New Metaheuristic Bat-Inspired Algorithm. In: *Nature Inspired Cooperative Strategies for Optimization (NICSO 2010)*, Gonzalez, J.R., D.A. Pelta, C. Cruz, G. Terrazas and N. Krasnogor (Eds.). Springer, Berlin, Germany, ISBN:978-3-642-12537-9, pp: 65-74.